Solving third-order Lane–Emden–Fowler equations using a variable stepsize formulation of a pair of block methods

Mufutau Ajani Rufai [a,*], Higinio Ramos [b,c]

[a] Dipartimento di Matematica, Università degli Studi di Bari Aldo Moro, 70125 Bari, Italy
[b] Scientific Computing Group, Universidad de Salamanca, Plaza de la Merced 37008 Salamanca, Spain
[c] Escuela Politécnica Superior de Zamora, Campus Viriato, 49022 Zamora, Spain

ABSTRACT

This manuscript presents a variable stepsize formulation of a pair of block methods to efficiently solve third-order IVP models of Lane–Emden–Fowler type equations. The main method is obtained considering two intermediate points. This method combines an appropriate set of formulas for dealing with the singularity at the left endpoint $t = 0$. The proposed method is implemented in variable stepsize mode to ensure that the truncation error is kept within a specified tolerance. The results of the numerical experiments confirm the good performance of the variable stepsize implementation presented in this paper.

© 2022 Elsevier B.V. All rights reserved.

1. Description of the problem

We are interested in solving Lane–Emden–Fowler type equations of the general form

$$u'''(t) = k(t, u(t), u'(t)) - g(t) \circ u'(t) - \frac{\lambda}{t} \circ u''(t), \tag{1}$$

$$u(0) = u_0, u'(0) = u'_0, \ u''(0) = u''_0, \quad t \in [0, t_N] \subset \mathbb{R}, u : [0, t_N] \to \mathbb{R}^d,$$

where u_0, u'_0, u''_0 and $\lambda = (\lambda_1, \ldots, \lambda_d) \in \mathbb{R}^d$ with $\lambda_i \geq 1$ are known, $g : [0, t_N] \to \mathbb{R}^d$, $k : [0, t_N] \times \mathbb{R}^{2d} \to \mathbb{R}^d$ are continuous functions, and $\circ$ denotes the Hadamard product. The theorems that guarantee the existence and uniqueness of solutions for this type of equations have been stated and proved in [1,2].

Singular models of this type have been used for modeling numerous real-world application problems in applied mathematics, astrophysics, dusty fluid systems, atomic nuclear reactions, chemical sciences, the theory of electromagnetic, quantum and classical mechanics, and mechanical and electrical engineering [3–5].

Due to the various practical applications of the problem under consideration, studying how to solve this problem analytically or numerically has been of great interest to numerous applied mathematicians, physicists, and engineering researchers.

Furthermore, due to the presence of the singularity at $t = 0$ and its nonlinear features, this is a complicated problem to solve exactly. Therefore, numerical approaches are often used to provide approximate and reasonable solutions.

---

* Corresponding author.
E-mail addresses: mufutau.rufai@uniba.it (M.A. Rufai), higra@usal.es (H. Ramos).

Numerous scholars have broadly examined the problem in (1) and given different approaches to provide a solution. To describe a few of the existing strategies in the accessible literature for integrating (1) and related singular problems, we can specify the variational iteration method in [6], the homotopy-perturbation method introduced by Chowdhury and Hashim [7], the neuro-swarming heuristics approach in [8], the analytical method in [9], the Adomian decomposition method and its modifications in [10–12], the differential transform approach described in [13], the Taylor series approach in [14], the quasilinearization technique in [15], the neural network algorithm based on integrated intelligent computing in [16], the Haar wavelet resolution technique in [17], the improved differential transform method reported in [18], the numerical methods in [19–24] or several approximation methods by spline functions in [25–30], and the references in those papers.

We clarify that most of the above strategies were implemented considering a fixed step size (FSS) mode. If the dynamics of the problem incorporate rapid changes in the solution, it is known that any numerical method with an FSS implementation is inefficient. For this reason, the authors of those papers presented results considering only very small stepsizes.

To address this shortcoming, we have considered a variable stepsize implementation using a pair of two-step hybrid block methods (PTSHBM) for solving (1) efficiently.

2. Mathematical formulation of the PTSHBM method

In this section we present the development of the PTSHBM.

2.1. Main formulas

To derive the PTSHBM, we assume that $d = 1$ and $t_j = t_0 + jh, j = 0, 1, \ldots, N$ with fixed stepsize $h = t_{j+1} - t_j$, and use a polynomial to approximate the true solution of problem (1), given by

$$u(t) \simeq q(t) = \sum_{j=0}^{7} c_j t^j. \tag{2}$$

From Eq. (2), we obtain

$$u'(t) \simeq q'(t) = \sum_{j=1}^{7} c_j j t^{j-1}, \tag{3}$$

$$u''(t) \simeq q''(t) = \sum_{j=2}^{7} c_j j(j-1) t^{j-2}, \tag{4}$$

$$u'''(t) \simeq q'''(t) = \sum_{j=3}^{7} c_j j(j-1)(j-2) t^{j-3}, \tag{5}$$

where the $c_j \in \mathbb{R}$ are unknown parameters that should be determined.

We define two distinctive middle points: $t_{n+r} = t_n + (1/4)h$ and $t_{n+s} = t_n + (7/4)h$ on $[t_n, t_{n+2}]$, and use the approximations in (2), (3) and (4) evaluated at the point t_n, and the third derivative approximation in (5) evaluated at the points $t_n, t_{n+r}, t_{n+1}, t_{n+s}, t_{n+2}$. In this way, the following system is obtained, with unknowns $c_n, n = 0(1)7$

$$q(t_n) = u_n, \, q'(t_n) = u'_n, \, q''(t_n) = u''_n, \, q'''(t_n) = w_n,$$
$$q'''(t_{n+r}) = w_{n+r}, \, q'''(t_{n+1}) = w_{n+1}, \, q'''(t_{n+s}) = w_{n+s}, \, q'''(t_{n+2}) = w_{n+2},$$

where $u_{n+j}, u'_{n+j}, u''_{n+j}$ and w_{n+j} give approximate values of $u(t_{n+j}), u'(t_{n+j}), u''(t_{n+j})$ and $u'''(t_{n+j})$, respectively, with w the right hand side in (1), that is, $w(t, u(t), u'(t), u''(t)) = k(t, u(t), u'(t)) - g(t)u'(t) - \dfrac{\lambda}{t} u''(t)$. Once we have obtained the values of $c_n, n = 0(1)7$, after using the substitution $t = t_n + xh$, the function $q(t)$ in (2) may be expressed as

$$q(t_n + xh) = \alpha_0(x)u_n + h\alpha_1(x)u'_n + h^2\alpha_2(x)u''_n \tag{6}$$
$$+ h^3 \left(\beta_0(x)w_n + \beta_r(x)w_{n+r} + \beta_1(x)w_{n+1} + \beta_s(x)w_{n+s} + \beta_2(x)w_{n+2} \right),$$

where the coefficients are given by

$$\alpha_0(x) = 1,$$
$$\alpha_1(x) = x,$$
$$\alpha_2(x) = x^2,$$
$$\beta_0(x) = \frac{4x^7}{735} - \frac{x^6}{21} + \frac{9x^5}{56} - \frac{85x^4}{336} + \frac{x^3}{6},$$

$$\beta_r(x) = -\frac{64x^7}{6615} + \frac{76x^6}{945} - \frac{232x^5}{945} + \frac{8x^4}{27},$$

$$\beta_1(x) = \frac{8x^7}{945} - \frac{8x^6}{135} + \frac{71x^5}{540} - \frac{7x^4}{108},$$

$$\beta_s(x) = -\frac{64x^7}{6615} + \frac{52x^6}{945} - \frac{88x^5}{945} + \frac{8x^4}{189},$$

$$\beta_2(x) = \frac{4x^7}{735} - \frac{x^6}{35} + \frac{13x^5}{280} - \frac{x^4}{48}.$$

Evaluating Eq. (6) together with its first and second derivatives at $x = 2$, we get

$$u_{n+2} = u_n + 2hu'_n + 2h^2 u''_n + \frac{h^3}{6615} \left(513w_n + 5248w_{n+r} + 3052w_{n+1}\right)$$

$$+ \frac{h^3}{6615} \left(-128w_{n+s} + 135w_{n+2}\right),$$

$$u'_{n+2} = u'_n + 2hu''_n + \frac{2h^2}{945} \left(27w_n + 64\left(7w_{n+r} + w_{n+s}\right) + 406w_{n+1}\right),$$

$$u''_{n+2} = u''_n + \frac{h}{945} \left(27w_n + 512\left(w_{n+r} + w_{n+s}\right) + 812w_{n+1} + 27w_{n+2}\right), \tag{7}$$

where $r = \frac{1}{4}$, $s = \frac{7}{4}$. We also evaluate $q(t)$, $q'(t)$ and $q''(t)$ at t_{n+r}, t_{n+1}, t_{n+s}, to get another nine formulas which will be combined with the ones in (7) to give the proposed two-step hybrid block method.

2.2. Strategy to circumvent the singularity

Because of the singularity at $t_0 = 0$, the main and additional formulas cannot be utilized to give approximate solutions to (1), since it is not possible to get $w_0 = w(t_0, u_0, u'_0, u''_0)$. In order to overcome the issue at $t_0 = 0$, we proceed to derive another hybrid block method for the subinterval $[t_0, t_2]$ using a similar procedure as the one presented above, but without considering the value of w_0. Now, the approximating polynomial is given by

$$u(t) \simeq \bar{q}(t) = \sum_{j=0}^{6} \bar{c}_j \, t^j. \tag{8}$$

Doing this, we get the formulas

$$u_2 = u_0 + 2hu'_0 + 2h^2 u''_0 - \frac{2h^3}{45} \left(-46w_{\bar{r}} + 39w_1 - 30w_{\bar{s}} + 7w_2\right), \tag{9}$$

$$u'_2 = u'_0 + 2hu''_0 - \frac{2h^2}{45} \left(-52w_{\bar{r}} + 36w_1 - 36w_{\bar{s}} + 7w_2\right),$$

$$u''_2 = u''_0 - \frac{2h}{3} \left(-2w_{\bar{r}} + w_1 - 2w_{\bar{s}}\right),$$

where $\bar{r} = \frac{1}{2}$, $\bar{s} = \frac{3}{2}$. We also obtain the remaining nine formulas by evaluating $\bar{q}(t)$, $\bar{q}'(t)$ and $\bar{q}''(t)$ at $t_{n+\bar{r}}$, t_{n+1}, $t_{n+\bar{s}}$.

3. Theoretical analysis of the PTSHBM

The theoretical analysis of the introduced technique PTSHBM is addressed in this section.

3.1. Order of accuracy and consistency of the PTSHBM

The formulas in (7) and additional nine formulas may be written as

$$\bar{A}_1 V_n = h \bar{A}_2 V'_n + h^2 \bar{A}_3 V''_n + h^3 \bar{A}_4 W_n, \tag{10}$$

where $\bar{A}_1, \bar{A}_2, \bar{A}_3, \bar{A}_4$ are coefficient matrices obtained from the formulas in (7) and the additional ones, with

$$V_n = (u_n, u_{n+r}, u_{n+1}, u_{n+s}, u_{n+2})^\top,$$

$$V'_n = \left(u'_n, u'_{n+r}, u'_{n+1}, u'_{n+s}, u'_{n+2}\right)^\top,$$

$$V''_n = \left(u''_n, u''_{n+r}, u''_{n+1}, u''_{n+s}, u''_{n+2}\right)^\top,$$

$$W_n = (w_n, w_{n+r}, w_{n+1}, w_{n+s}, w_{n+2})^\top.$$

We assume that $u(t)$ is sufficiently differentiable and consider the operator $\mathcal{L}$ related to the formulas in (7):

$$\mathcal{L}(u(t); h) = \sum_{j \in I} \left[\alpha_j u(t + jh) - h\beta_j u'(t + jh) - h^2 \gamma_j u''(t + jh) \right.$$
$$\left. -h^3 v_j u'''(t + jh) \right], \tag{11}$$

where $\alpha_j, \beta_j, \gamma_j$ and v_j are respectively vector columns of $\bar{A}_1, \bar{A}_2, \bar{A}_3, \bar{A}_4$, and I is a set of indices given by $I = \{0, r, 1, s, 2\}$. Using the Taylor series expansion we get

$$\mathcal{L}(u(t); h) = C_0 u(t) + C_1 h u'(t) + C_2 h^2 u''(t) + C_3 h^3 u'''(t) + \cdots + C_q h^q u^q(t) + \ldots, \tag{12}$$

where

$$C_q = \frac{1}{q!} \left[\sum_{j \in I}^{k} j^q \alpha_j - q \sum_{j \in I}^{k} j^{q-1} \beta_j - q(q-1) \sum_{j \in I}^{k} j^{q-2} \gamma_j \right.$$
$$\left. -q(q-1)(q-2) \sum_{j \in I}^{k} j^{q-3} v_j \right], \tag{13}$$

and $q = 0, 1, 2, \ldots$.

The preceding operator associated to the formulas in (7) and additional ones is called to be of order p if $C_0 = C_1 = \cdots = C_{p+1} = C_{p+2} = 0, C_{p+3} \neq 0$. The C_{p+3} contains the principal terms of the local truncation errors (LTE). Using this we get the order (p) of the main formulas and their LTEs, given by

$$p = 5, \qquad \mathcal{L}(u(t_{n+2}); h) = -\frac{h^8 u^{(8)}(t_n)}{3360} + \mathcal{O}(h^9)$$
$$p = 5, \qquad \mathcal{L}(u'(t_{n+2}); h) = -\frac{h^7 u^{(8)}(t_n)}{3360} + \mathcal{O}(h^8)$$
$$p = 6, \qquad \mathcal{L}(u''(t_{n+2}); h) = \frac{h^7 u^{(9)}(t_n)}{20160} + \mathcal{O}(h^8). \tag{14}$$

We further get the order (p) of the specific formulas in (9) and their local truncation errors. We obtain

$$p = 4, \qquad \mathcal{L}(u(t_2); h) = \frac{31}{1680} \left(h^7 u^{(7)}(t_0) \right) + \mathcal{O}(h^8)$$
$$p = 4, \qquad \mathcal{L}(u'(t_2); h) = \frac{7}{360} \left(h^6 u^{(7)}(t_0) \right) + \mathcal{O}(h^7)$$
$$p = 4, \qquad \mathcal{L}(u''(t_2); h) = \frac{7}{720} \left(h^5 u^{(7)}(t_0) \right) + \mathcal{O}(h^6). \tag{15}$$

Since the formulas have an order greater than one, then they are consistent.

3.2. Zero-stability of the PTSHBM

Zero-stability of the PTSHBM is associated with the behavior of Eq. (10), when $h \to 0$. As $h \to 0$, (10) may be rewritten as

$$K_1^{(0)} \bar{V}_\mu - K_1^{(1)} \bar{V}_{\mu-1} = 0,$$

where

$$\bar{V}_\mu = (u_{n+2}, u_{n+s}, u_{n+1}, u_{n+r})^\top, \qquad \bar{U}_{\mu-1} = (u_n, u_{n+s-2}, u_{n-1}, u_{n+r-2})^\top,$$

$$K_1^{(0)} = \begin{pmatrix} 1 & 0 & 0 & 0 \\ 0 & 1 & 0 & 0 \\ 0 & 0 & 1 & 0 \\ 0 & 0 & 0 & 1 \end{pmatrix}, \qquad K_1^{(1)} = \begin{pmatrix} 1 & 0 & 0 & 0 \\ 1 & 0 & 0 & 0 \\ 1 & 0 & 0 & 0 \\ 1 & 0 & 0 & 0 \end{pmatrix}.$$

The PTSHBM is zero-stable if the roots r_j of its first characteristic polynomial $P(r)$ expressed by $P(r) = \det \left[K_1^{(0)} r - K_1^{(1)} \right]$, fulfill $|r_j| \leq 1$, and those roots with $|r_j| = 1$ have multiplicities which are not greater than 2 (see [31]). Since $P(r) = (r-1)r^3$, the PTSHBM is zero-stable.

3.3. Convergence analysis

Although zero-stability and consistency of the proposed formulas determine the convergence of the block method, the theoretical order of convergence will be analyzed here. To do this we consider the block method as a global one given by the formulas obtained in Section 2.2 together with the formulas obtained in Section 2.1 for $n = 2, 4 \ldots, N - 2$.

Theorem 3.1 (*Convergence Theorem*). [32] *Let* $u(t)$ *denote the true solution to problem* (1) *and* $\{u_j\}_{j=1}^N$ *the discrete solution provided by the proposed method. Then the proposed method is convergent of order six.*

Following [32,33], we denote the $6N$-vector of approximate values as follows

$$\bar{U} = \left(u_{\bar{r}}, u_1, \ldots, u_N, u_{\bar{r}}', \ldots, u_N', u_{\bar{r}}'', \ldots, u_N'' \right)^T,$$

and the $2N$-vector of approximate values of the function w by

$$\bar{W} = (w_{\bar{r}}, w_1, w_{\bar{s}}, w_2, w_{2+r}, \ldots, w_{N-2+s}, w_N)^T.$$

Consider the square matrix D of dimension $6N$ containing the coefficients that multiply the terms in $\bar{U}$, and V the matrix of dimension $6N \times 2N$ containing the coefficients that multiply the terms in $\bar{W}$, in the formulas of the method. This results in the following system

$$D\bar{U} + hV\bar{W} + C = 0 \tag{16}$$

where C is a $6N$-vector of the known values (related to the initial values). This system approximates the solution and its first and second derivatives at each grid point and at the intermediate points. If we now take the vectors of exact values corresponding to U and W, as follows

$$U = \left(u(t_{\bar{r}}), \ldots, u(t_N), u'(t_{\bar{r}}), \ldots, u'(t_N), u''(t_{\bar{r}}), \ldots, u''(t_N) \right)^T,$$

$$W = \left((w(t_{\bar{r}}, u(t_{\bar{r}}), u'(t_{\bar{r}}), u''(t_{\bar{r}})), w(t_1, u(t_1), u'(t_1), u''(t_1)), \ldots, w(t_N, u(t_N), u'(t_N), u''(t_N))) \right)^T,$$

we obtain the following system

$$DU + hVW + C = L, \tag{17}$$

where L is the $6N$-vector of the local truncation errors of the formulas in the proposed method, given by

$$L \simeq \begin{bmatrix} \mathcal{L}[u(t_{\bar{r}}), h] \\ \mathcal{L}[u(t_1), h] \\ \ldots \\ \mathcal{L}[u(t_N), h] \\ \mathcal{L}[u'(t_{\bar{r}}), h] \\ \mathcal{L}[u'(t_1), h] \\ \ldots \\ \mathcal{L}[u'(t_N), h] \\ \mathcal{L}[u''(t_{\bar{r}}), h] \\ \mathcal{L}[u''(t_1), h] \\ \ldots \\ \mathcal{L}[u''(t_N), h] \end{bmatrix}.$$

By subtracting (16) from (17) we get

$$DE_{error} + hV(W - \bar{W}) = L, \tag{18}$$

where $E_{error} = U - \bar{U} = \left(e_{\bar{r}}, \ldots, e_N, e_{\bar{r}}', \ldots, e_N', e_{\bar{r}}'', \ldots, e_N'' \right)^T$ is the $6N$-vector of errors at the grid and intermediate points of the solution and its first and second derivatives. By utilizing the Mean Value Theorem [34], one can take into consideration at each index the identities

$$w(t_i, u(t_i), u'(t_i), u''(t_i)) - w(t_i, u_i, u_i', u_i'') = (u(t_i) - u_i) \frac{\partial w}{\partial u} (\xi_i)$$

$$+ \left(u'(t_i) - u_i' \right) \frac{\partial w}{\partial u'} (\xi_i)$$

$$+ \left(u''(t_i) - u_i'' \right) \frac{\partial w}{\partial u''} (\xi_i),$$

where ξ_i denotes an intermediate point in the line between $(t_i, u(t_i), u'(t_i), u''(t_i))$ and (t_i, u_i, u'_i, u''_i). In view of the above we can put

$$
(W - \bar{W}) = \begin{pmatrix} \frac{\partial w}{\partial u}(\xi_{\bar{r}}) & \dots & 0 & \frac{\partial w}{\partial u'}(\xi_{\bar{r}}) & \dots & 0 & \frac{\partial w}{\partial u''}(\xi_{\bar{r}}) & \dots & 0 \\ 0 & \dots & 0 & 0 & \dots & 0 & 0 & \dots & 0 \\ . & \dots & . & . & \dots & . & . & \dots & . \\ . & \dots & . & . & \dots & . & . & \dots & . \\ . & \dots & . & . & \dots & . & . & \dots & . \\ 0 & \dots & \frac{\partial w}{\partial u}(\xi_N) & 0 & \dots & \frac{\partial w}{\partial u'}(\xi_N) & 0 & \dots & \frac{\partial w}{\partial u''}(\xi_N) \end{pmatrix} \begin{pmatrix} e_{\bar{r}} \\ \vdots \\ e_N \\ e'_{\bar{r}} \\ \vdots \\ e'_N \\ e''_{\bar{r}} \\ \vdots \\ e''_N \end{pmatrix}
$$

$$
= J_w E_{error}.
$$

The equation in (18) can be expressed as follows:

$$
(D + hVJ_w) E_{error} = L,
$$

and thus

$$
E_{error} = (D + hVJ_w)^{-1} L.
$$

Expanding each term of $(D + hVJ_w)^{-1}$ in powers of h it can be shown after tedious manipulations (see [35]) that the maximum norm verifies

$$
\| (D + hVJ_w)^{-1} \| = |O(h)|.
$$

Finally, having in mind the formulas of the local truncation errors, we get

$$
\|E_{error}\| = |O(h)||O(h^5)| < Kh^6,
$$

showing that the proposed method exhibits a sixth-order convergence.

3.4. Linear stability of the PTSHBM

We studied the generalized linear stability of the PTSHBM through the application of the method in (10) to the test problem

$$
u'''(t) = -3\mu u''(t) - 3\mu^2 u'(t) - \mu^3 u(t), \quad \Re(\mu) > 0, \tag{19}
$$

where μ indicates a complex parameter and the above equation has bounded solutions that go to zero as t tends to infinity. Employing the PTSHBM with the test Eq. (19) we have

$$
R \begin{pmatrix} u_r \\ u_1 \\ u_s \\ u_2 \\ u'_r \\ u'_1 \\ u'_s \\ u'_2 \\ u''_r \\ u''_1 \\ u''_s \\ u''_2 \end{pmatrix} = S \begin{pmatrix} u_{r-2} \\ u_{1-2} \\ u_{s-2} \\ u_0 \\ u'_{r-2} \\ u'_{1-2} \\ u'_{s-2} \\ u'_0 \\ u''_{r-2} \\ u'_{1-2} \\ u'_{s-2} \\ u''_0 \end{pmatrix},
$$

where R and S are the matrix coefficients of the formulas given in (10). By letting $z = \mu h$, we examine the stability of the proposed PTSHBM through the eigenvalues of the amplification matrix ($M(z) = R^{-1}S$). The obtained stability region of the proposed PTSHBM using the above test equation is represented in Fig. 1.
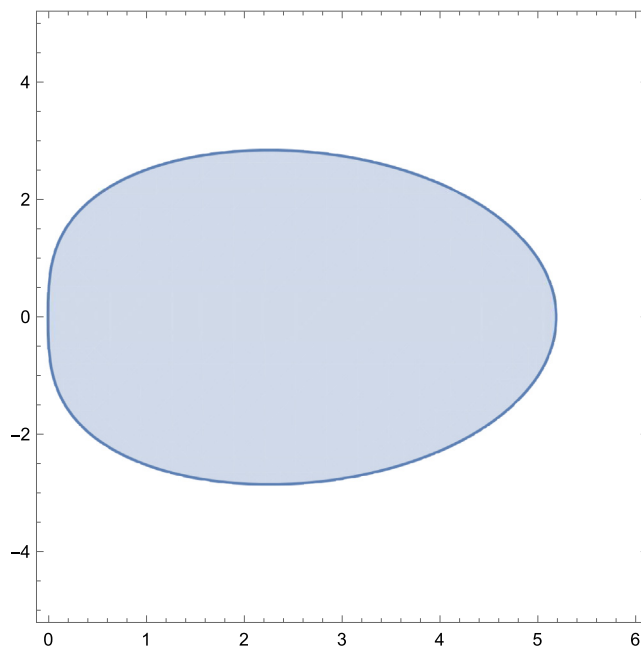
Fig. 1. Stability region in the complex z-plane using the test Eq. (19).

4. Error estimation of the PTSHBM

Here, we provide a variable step size formulation of the PTSHBM. This formulation is interesting since it allows the use of large integration steps. At the same time, most of the existing numerical methods in the literature for solving this kind of problem are not formulated in variable stepsize mode. Our goal is to guarantee that the truncation error is maintained within a specified tolerance. In this paper, an embedding strategy is used to formulate the proposed method in variable stepsize mode, which means that apart from the approximation for u_{n+2}, we will also need an additional lower order method (LOM) approximation for u^*_{n+2}. A difference between the u_{n+2} and u^*_{n+2} approximations will provide a local error estimation. The following formula:

$$u^*_{n+2} = 7u_n + \frac{14u_{n+1}}{3} - \frac{32u_{n+r}}{3} + \frac{1}{864}h^3 \left(-54w_n + 322w_{n+1} + 217w_{n+r} + 19w_{n+s}\right), \qquad (20)$$

with local truncation error $LTE = \frac{227}{737280} h^7 u^{(7)}(t_n) + O\left(h^7\right)$ has been used to estimate the local error through the difference

$$ERREST = \|u_{n+2} - u^*_{n+2}\|. \qquad (21)$$

Given a tolerance, TOL, if $|ERREST| \le TOL$, the obtained approximations are accepted, we take $h_{vary} = 2 \times h_{old}$, and proceed with the computations with h_{vary} by assuming that $h_{minimum} \le h_{vary} \le h_{maximum}$. If $|ERREST| > TOL$, then obtained values are rejected and we repeat the computations using the following strategy for changing the step size:

$$h_{vary} = \lambda \, h_{old} \left(\frac{TOL}{\|ERREST\|}\right)^{1/(p+3)}, \qquad (22)$$

where $p = 4$ is the order of the LOM in (20) and $\lambda = 0.9$ is a suitable adjustment factor.

5. Notes on the implementation

The PTSHBM is executed using the strategy in the above section. The systems in (7) and additional formulas has been expressed in the form $\boldsymbol{W(u) = 0}$, with unknowns

$$\tilde{\mathbf{U}} = \left\{u_{\bar{r}}, u_1, u_{\bar{s}}, u'_{\bar{r}}, u'_1, u'_{\bar{s}}, u''_{\bar{r}}, u''_1, u''_{\bar{s}}\right\} \bigcup \{u_j\}_{j=2,4,\ldots,N} \bigcup \{u'_j\}_{j=2,4,\ldots,N} \bigcup \{u''_j\}_{j=2,4,\ldots,N}$$

$$\bigcup \left\{u_{j+r}, u_{j+1}, u_{j+s}, u'_{j+r}, u'_{j+1}, u'_{j+s}, u''_{j+r}, u''_{j+1}, u''_{j+s}\right\}_{j=2,4,\ldots,N-2}.$$

Since the PTSHBM is an implicit method, we consider a Modified Newton's method (MNM) to solve the obtained system of non-linear equations. The MNM is given by

$$\tilde{\mathbf{U}}^{i+1} = \tilde{\mathbf{U}}^i - (\mathbf{J_0})^{-1} \mathbf{W}^i,$$

where $\mathbf{J_0}$ represents the frozen jacobian matrix of $\mathbf{W}$. The following formulas are used to initialize the MNM on each iteration

$$u_{n+i} = u_n + (ih)u'_n + \frac{(ih)^2}{2}u''_n + \frac{(ih)^3}{6}w_n,$$

$$u'_{n+i} = u'_n + (ih)u''_n + \frac{(ih)^2}{2}w_n,$$

$$u''_{n+i} = u''_n + (ih)w_n,$$

for $n = 0, i = \bar{r}, 1, \bar{s}, 2$ and $n = 2, 4 \ldots, N-2, i = r, 1, s, 2$.

5.1. Algorithm for solving (1)

Data: Initialize starting algorithm: $h = h_0 = h_{old}, t_m := t_0, u_m := u_0$;
       Total number of steps in the main method: $N-2$;
       End-point of the integration interval: t_N
Result: Approximations of the problem in (1) at selected points.
1 Introduce $w(t, u(t), u'(t), u''(t))$ and initial values u_0, u'_0, u''_0;
3 Use the ad-hoc formulas in (9) with $h = h_0$ to get the values $u_1, u_2, u'_1, u'_2, u''_1, u''_2$.
5 Set m=2.
7 If $t_m \geq t_N$, then exit.
9 If $t_m + 2h > t_N$, then $h = (t_N - t_m)/2$.
11 **While** $t_m < t_N$ **do** use the main strategy taking $h = h_{old}$ to get the values $u_{m+1}, u_{m+2}, u'_{m+2}, u''_{m+2}$;
13 Compute u^*_{m+2} to get $ERREST = \|u_{m+2} - u^*_{m+2}\|$.
15 **If** $|ERREST| \leq TOL$, **then** accept the results and put $h_{vary} = 2 \times h_{old}$.
17 Set $t_m = t_m + 2h, m = m + 2$ and go to step **11**.
19 **If** $|ERREST| > TOL$, **then** we repeat the computations using (22) and go to step **11**.
20 **end**

---

6. Numerical Experiments

In this section, we evaluate the performance of the PTSHBM by considering some numerical experiments. In the presented Tables and Figures, we have utilized the abbreviations:

- PTSHBM : The pair of two-step hybrid block methods in this paper.
- UHWRT: The uniform Haar wavelet resolution technique in [17].
- CBSAM: A cubic B-spline approximation method in [2].
- RKHSM: The reproducing kernel Hilbert space method in [36].
- IICPM: An Integrated intelligent computing paradigm method in [37].
- NS: Number of steps.
- NJ: Number of Jacobians.
- MNI: Number of Newton iterations.
- FE: Total number of function evaluations.
- MAXAE: Maximum absolute errors.
- h_0 : Initial step.
- TOL: Predefined tolerance.
- CPU: The computational time in seconds.

6.1. Numerical Experiment 1

We firstly consider the following problem [2,36]

$$u'''(t) = \frac{2}{t}u''(t) + \frac{9\left(t^6 + 8\right)}{8u(t)^5},$$

$$u(0) = 1, \quad u'(0) = 0, \quad u''(0) = 0, \quad t \in [0, t_N], \tag{23}$$

whose exact solution is $u(t) = \sqrt{1 + t^3}$.

The numerical results for the proposed PTSHBM reported in Table 1 were obtained by taking $TOL = 10^{-5}, h_0 = 10^{-2}$ and $TOL = 10^{-9}, h_0 = 10^{-2}$, respectively. Not only is the proposed technique the one that gives the best accuracy, but it also has the lowest number of steps, being the most efficient of the methods considered.

Table 1
Comparison of the numerical results for problem (23) on $t \in [0, 1]$.

Method	NS	MAXAE
PTSHBM	9	3.6568×10^{-6}
CBSAM	10	5.2500×10^{-5}
RKHSM	20	7.7839×10^{-6}
PTSHBM	21	1.6962×10^{-9}
CBSAM	40	5.1900×10^{-7}
RKHSM	35	4.3964×10^{-6}

6.2. Numerical Experiment 2

We also consider the following problem that has appeared in [2,36]

$$u'''(t) = 6\left(t^6 + 2t^3 + 10\right)e^{-3u(t)} - \frac{6}{t^2}u'(t) - \frac{6}{t}u''(t),$$

$$u(0) = 0, \quad u'(0) = 0, \quad u''(0) = 0, \quad t \in [0, t_N]. \tag{24}$$

The exact solution of this problem is $u(t) = \log\left(1 + t^3\right)$.

The numerical results of the proposed PTSHBM for problem (24) reported in Table 3 were obtained by taking $TOL = 10^{-6}$, $h_0 = 10^{-3}$ and $TOL = 10^{-8}$, $h_0 = 10^{-3}$, respectively. Not only the introduced technique is the one that provides the most reliable efficiencies, but it gives the lowest NS, being the most effective of the approaches considered.

6.3. Numerical Experiment 3

Consider the following problem [6,37]

$$u'''(t) + \frac{8}{t}u''(t) + \frac{12}{t^2}u'(t) + u(t)^m = 0, \quad m = 0,$$

$$u(0) = 1, \quad u'(0) = 0, \quad u''(0) = 0, \quad t \in [0, t_N], \tag{25}$$

whose exact solution is $u(t) = 1 - \frac{t^3}{90}$.

The reported range of AE for IICPM is $10^{-09} - 10^{-07}$, while for the PTSHBM, the range of AE plotted in Fig. 4 is $10^{-16} - 10^{-17}$, showing the better performance of the proposed PTSHBM.

6.4. Numerical Experiment 4

Consider the following system

$$u_1''' + \frac{u_1''}{t} - \frac{u_1'}{t^2} - u_2^2\left(2u_1u_2u_1' + 3\left(u_1^2 + 1\right)u_2'\right) = 0,$$

$$u_1''' + \frac{3u_2''}{t} - \frac{3u_2'}{t^2} + u_2^4\left(2u_1u_2u_1' + 5\left(u_1^2 + 3\right)u_2'\right) = 0,$$

$$u_1''' - \frac{3\left(u_3' - tu_3''\right)}{t^2} - 4t^3u_2^7 - 7t^4u_2^6u_2' + 5u_2^4\left(u_3^2 - 6\right)u_2'$$

$$+ 2u_2^5\left(6u_2' + u_3u_3'\right) = 0, \quad t \in [0, t_N], \tag{26}$$

with initial values

$$u_1(0) = 1, \quad u_1'(0) = 0, \quad u_1''(0) = 1,$$

$$u_2(0) = 1, \quad u_2'(0) = 0, \quad u_2''(0) = -1,$$

$$u_3(0) = 0, \quad u_3'(0) = 0, \quad u_3''(0) = 1.$$

The exact solution is:

$$u_1(t) = \sqrt{1 + t^2}, \qquad u_2(t) = \frac{1}{\sqrt{1 + t^2}}, \qquad u_3(t) = 1 - \frac{1}{\sqrt{1 + t^2}}.$$

We have used the PTSHBM to solve problem (23) with $t \in [0, 100]$, problem (24) with $t \in [0, 100\pi]$, problem (25) with $t \in [0, 2000]$, and problem (26) with $t \in [0, 10\pi]$. Tables 1–7 and Figs. 2–7 show good numerical results obtained with the PTSHBM scheme when solving problems (23)–(26).
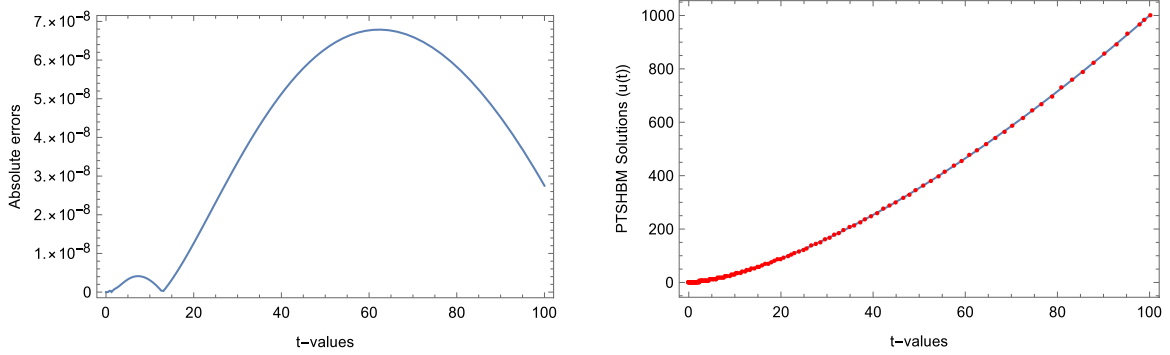
Fig. 2. Errors (left), and exact solution and PTSHBM approximation (right) for (23) (TOL = 10^{-10}, $h_0 = 10^{-2}$, $t \in [0, 100]$).
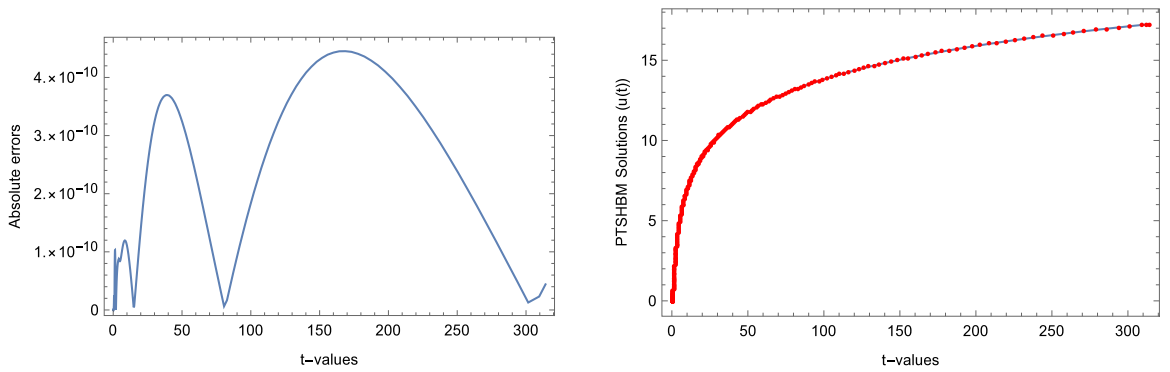

Fig. 3. Errors (left), and exact solution and PTSHBM approximation (right) for (24) (TOL = 10^{-11}, $h_0 = 10^{-3}$, $t \in [0, 100\pi]$).
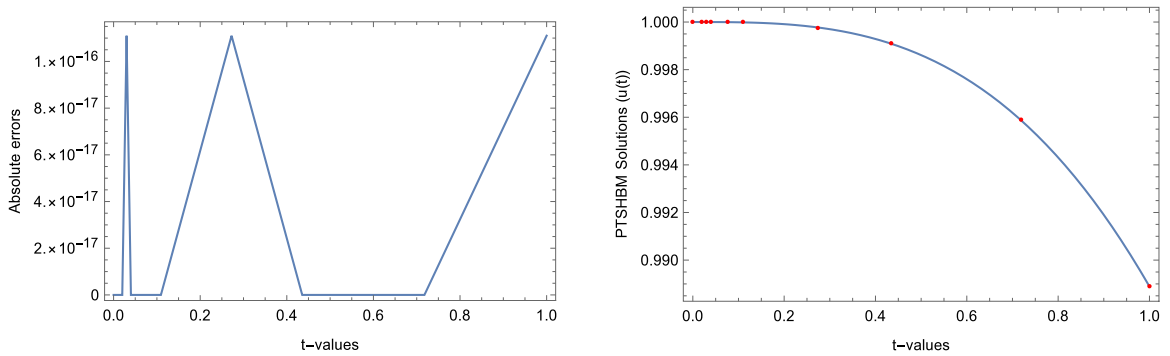

Fig. 4. Errors (left), and exact solution and PTSHBM approximation (right) for (25) (TOL = 10^{-12}, $h_0 = 10^{-2}$, $t \in [0, 1]$).
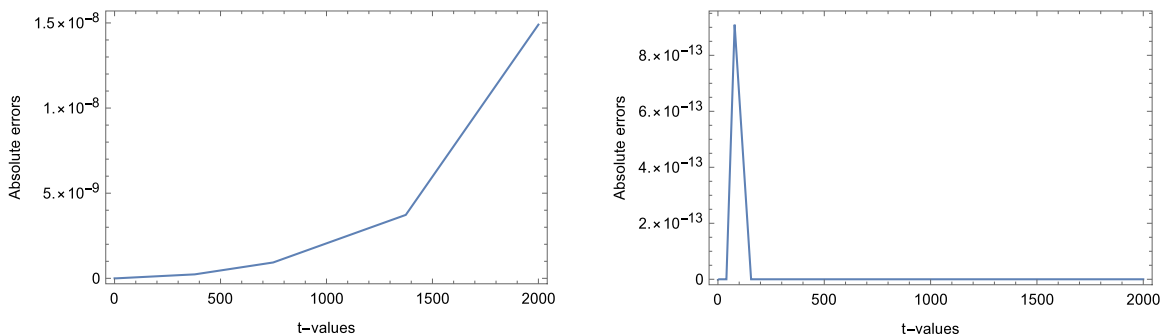

Fig. 5. Absolute errors for data in Table 6.

Table 2
Numerical results on (23) with $h_0 = 10^{-2}, t \in [0, 100]$.

TOL	Method	NS	NJ	MNI	FE	CPU	MAXAE
10^{-8}	PTSHBM	83	47	102	209	0.1353	2.9190×10^{-6}
10^{-10}	PTSHBM	149	83	175	374	0.2371	6.7865×10^{-8}
10^{-12}	PTSHBM	291	194	392	729	0.5017	4.0714×10^{-9}

Table 3
Comparison of the numerical results for problem (24) on $t \in [0, 1]$.

Method	NS	MAXAE
PTSHBM	15	1.7152×10^{-7}
CBSAM	20	5.5500×10^{-6}
RKHSM	30	2.8567×10^{-6}
PTSHBM	23	1.5096×10^{-8}
CBSAM	40	4.0800×10^{-7}
RKHSM	45	1.2923×10^{-6}

Table 4
Numerical results for problem (24) with $h_0 = 10^{-3}, t \in [0, 100\pi]$.

TOL	Method	NS	NJ	MNI	FE	CPU	MAXAE
10^{-9}	PTSHBM	141	79	179	354	0.3212	1.3918×10^{-8}
10^{-11}	PTSHBM	259	144	308	649	0.5566	4.4519×10^{-10}
10^{-13}	PTSHBM	483	293	606	1209	1.1598	1.1598×10^{-11}

Table 5
Numerical results for problem (25) with TOL = $10^{-6}, h_0 = 10^{-2}, t \in [0, 1]$.

t	Exact	OHBNTM	AE
0	1.0000000000000000	1.0000000000000000	0.0000
0.02	1.0000000000000000	0.9999999111111111	0.0000
0.03	0.9999997000000000	0.9999996999999999	1.1102×10^{-16}
0.04	0.9999992888888889	0.9999992888888889	0.0000
0.52	0.9984376888888888	0.9984376888888890	1.1102×10^{-16}
1.00	0.9888888888888889	0.9888888888888888	1.1102×10^{-16}

Table 6
Numerical results for problem (25) with $h_0 = 10^{-2}, t \in [0, 2000]$.

TOL	Method	NS	NJ	MNI	FE	CPU	MAXAE
10^{-4}	PTSHBM	11	5	5	29	0.0230	1.4901×10^{-8}
10^{-6}	PTSHBM	13	6	6	34	0.0252	9.0949×10^{-13}

Table 7
Numerical results on (26) with $h_0 = 10^{-2}, t \in [0, 10\pi]$.

TOL	Method	NS	NJ	MNI	FE	CPU	MAXAE
10^{-9}	PTSHBM	73	41	120	184	2.1019	16525×10^{-4}
10^{-10}	PTSHBM	97	53	155	244	2.8071	1.8048×10^{-5}
10^{-11}	PTSHBM	131	72	212	329	3.7258	5.9320×10^{-7}

7. Concluding remarks

In this article, a variable stepsize formulation of a pair of two-step block methods (PTSHBM) is developed and efficiently applied for getting more reliable approximations to the Lane–Emden–Fowler model equations presented in (1). The developed PTSHBM is implemented in a variable stepsize mode by adapting the number and position of the nodes utilized in the approximation to assure that the truncation errors are maintained within a specified bound. The reliable and accurate performance is observed for PTSHBM based on an estimate of the error and the adaptive strategy provided in this manuscript. Numerical results in Tables 1–7 and Figs. 2–7 confirm that the proposed method is more efficient for solving problem (1) than other existing numerical methods. For future research work, we note the study on
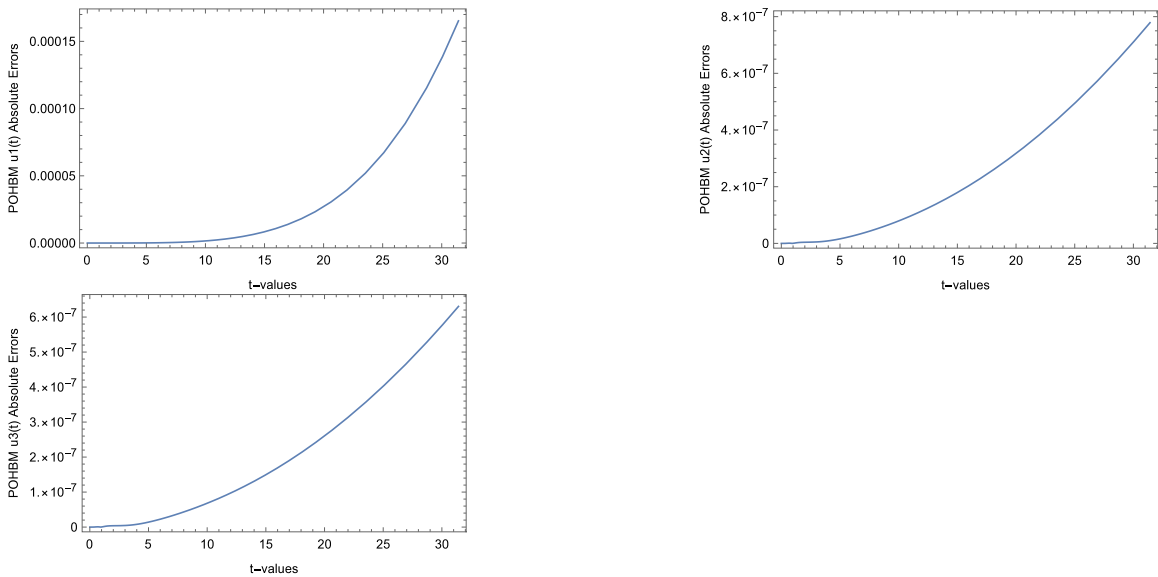
Fig. 6. Absolute errors for (26) (TOL = 10^{-9}, $h_0 = 10^{-2}$, $t \in [0, 10\pi]$).
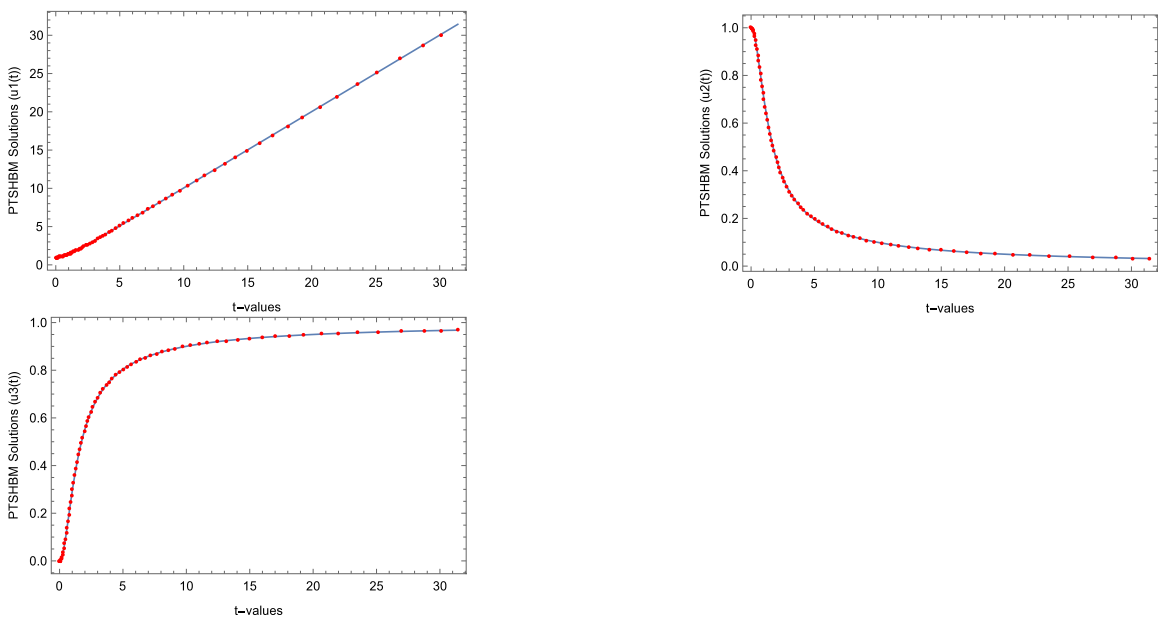

Fig. 7. PTSHBM approximations for (26) (TOL = 10^{-9}, $h_0 = 10^{-2}$, $t \in [0, 10\pi]$).

how to apply the proposed method for solving time-dependent partial and fractional-order differential equations of the Lane–Emden–Fowler type.

Data availability

No data was used for the research described in the article.

References

[1] D.C. Biles, M.P. Robinson, J.S. Spraker, A generalization of the lane-Emden equation, J. Math. Anal. Appl. 273 (2002) 654–666.
[2] K.I. Muhammad, A. Muhammad, W. Imtiaz, New cubic B-spline approximation for solving third order Emden-fowler type equations, Appl. Math. Comput. 331 (2018) 319–333.

[3] P. Rosenau, A note on integration of the Emden-fowler equation, Int. J. Non-Linear Mech. 19 (1984) 303–308.

[4] M.A. Rufai, H. Ramos, Numerical solution of second-order singular problems arising in astrophysics by combining a pair of one-step hybrid block Nyström methods, Astrophys. Space Sci. 365 (2020) 96.

[5] K. Thula, P. Roul, A high-order B-spline collocation method for solving nonlinear singular boundary value problems arising in engineering and applied science, Mediterr. J. Math. 15 (2018) 176.

[6] A.M. Wazwaz, Solving two Emden–Fowler type equations of third order by the variational iteration method, Appl. Math. 9 (5) (2015) 2429–2436.

[7] M.S.H. Chowdhury, I. Hashim, Solution of a class of singular second-order IVPs by homotopy-perturbation method, Phys. Lett. A 365 (2007) 439–447.

[8] Z. Sabir, M.A.Z. Raja, M. Umar, Design of neuro-swarming-based heuristics to solve the third-order nonlinear multi-singular Emden–Fowler equation, Eur. Phys. J. Plus 135 (2020) 410.

[9] G. Adomian, R. Rach, N.T. Shawagfeh, On the analytic solution of the lane-Emden equation, Found. Phys. Lett. 8 (1995) 161–181.

[10] A.M. Wazwaz, A new algorithm for solving differential equations of lane–Emden type, Appl. Math. Comput. 118 (2) (2001) 287–310.

[11] A.M. Wazwaz, Randolph Rach, Jun-Sheng Duan, Adomian decomposition method for solving the Volterra integral form of the lane–Emden equations with initial values and boundary conditions, Appl. Math. Comput. 219 (10) (2013) 5004–5019.

[12] Y.Q. Hasan, L.M. Zhu, A note on the use of modified adomian decomposition method for solving singular boundary value problems of higher-order ordinary differential equations, Commun. Nonlinear Sci. Numer. Simul. 14 (8) (2009) 3261–3265.

[13] K. Aruna, A.R. Kanth, A novel approach for a class of higher order nonlinear singular boundary value problems, Int. J. Pure Appl. Math. 84 (4) (2013) 321–329.

[14] J.H. He, F.Y. Ji, Taylor series solution for lane–Emden equation, J. Math. Chem. 57 (8) (2019) 1932–1934.

[15] V.B. Mandelzweig, F. Tabakin, Quasilinearization approach to nonlinear problems in physics with application to nonlinear ODEs, Comput. Phys. Comm. 141 (2) (2001) 268–281.

[16] M.A.Z. Raja, J. Mehmood, Z. Sabir, A.K. Nasab, M.A. Manzar, Numerical solution of doubly singular nonlinear systems using neural networks-based integrated intelligent computing, Neural Comput. Appl. 31 (3) (2019) 793–812.

[17] K. Swati, A.K. Verma, M. Singh, Higher order Emden–Fowler type equations via uniform haar wavelet resolution technique, J. Comput. Appl. Math. 376 (2020) 112836.

[18] L.J. Xie, C.L. Zhou, S. Xu, An effective numerical method to solve a class of nonlinear singular boundary value problems using improved differential transform method, Springer Plus 5 (1) (2016) 1066.

[19] R. Amin, K. Shah, M. Asif, I. Khan, A computational algorithm for the numerical solution of fractional order delay differential equations, Appl. Math. Comput. 402 (2021) 125863.

[20] R. Amin, K. Shah, M. Asif, I. Khan, F. Ullah, An efficient algorithm for numerical solution of fractional integro-differential equations via haar wavelet, J. Comput. Appl. Math. 381 (2021) 113028.

[21] H. Ramos, M.A. Rufai, An adaptive pair of one-step hybrid block Nyström methods for singular initial-value problems of lane-Emden-fowler type, Math. Comput. Simulation 193 (2022) 497–508.

[22] M.A. Rufai, H. Ramos, Numerical solution for singular boundary value problems using a pair of hybrid Nyström techniques, Axioms 10 (2021) 202.

[23] H. Ramos, M.A. Rufai, An adaptive one-point second-derivative lobatto-type method for solving efficiently differential systems, Int. J. Comput. Math. 99 (8) (2022) 1687–1705.

[24] Z. Sabir, M.A.Z. Raja, J.L. Guirao, T. Saeed, Meyer wavelet neural networks to solve a novel design of fractional order pantograph lane-Emden differential model, Chaos, Solitons Fract. 152 (2021) 111404.

[25] Y.A. Wakijira, G.F. Duressa, T.A. Bullo, Quintic non-polynomial spline methods for third order singularly perturbed boundary value problems, J. King Saud. Univ. Sci. 30 (2018) 131–137.

[26] N. Caglar, H. Caglar, B-spline solution of singular boundary value problems, Appl. Math. Comput. 182 (2) (2006) 1509–1513.

[27] M. Abukhaled, S.A. Khuri, A. Sayfy, A numerical approach for solving a class of singular boundary value problems arising in physiology, Int. J. Numer. Anal. Model. 8 (2) (2011) 353–363.

[28] A.R. Kanth, Cubic spline polynomial for non-linear singular two-point boundary value problems, Appl. Math. Comput. 189 (2) (2007) 2017–2022.

[29] S.A. Khuri, A. Sayfy, Numerical solution for the nonlinear Emden-fowler type equations by a fourth-order adaptive method, Int. J. Comput. Meth. 11 (1) (2014) 1350052.

[30] B. Lin, A new numerical scheme for third-order singularly Emden–Fowler equations using quintic B-spline function, Int. J. Comput. Math. 98 (12) (2021) 2406–2422.

[31] M.A. Rufai, H. Ramos, A variable step-size fourth derivative hybrid block strategy for integrating third-order IVPs, with applications, Int. J. Comput. Math. 99 (2) (2022) 292–308.

[32] M.A. Rufai, Higinio Ramos, Numerical integration of third-order singular boundary-value problems of Emden–Fowler type using hybrid block techniques, Commun. Nonlinear Sci. Numer. Simul. 105 (2022) 106069.

[33] H. Ramos, M.A. Rufai, Two-step hybrid block method with fourth derivatives for solving third-order boundary value problems, J. Comput. Appl. Math. 404 (2022) 113419.

[34] H. Dym, Linear Algebra in Action, AMS, Providence, Rhode Island, 2007.

[35] H. Ramos, G. Singh, Solving second order two-point boundary value problems accurately by a third derivative hybrid block integrator, Appl. Math. Comput. 421 (2022) 126960.

[36] A. Dezhbord, T. Lotfi, K. Mahdiani, A numerical approach for solving the high-order nonlinear singular Emden–Fowler type equations, Adv. Differential Equations 2018 (2018) 161.

[37] Z. Sabir, M. Umar, J.L.G. Guirao, M. Shoaib, M.A.Z. Raja, Integrated intelligent computing paradigm for nonlinear multi-singular third-order Emden–Fowler equation, Neural Comput. Appl. 33 (2021) 3417–3436.